JOURNAL OF SOLID STATE CHEMISTRY **42**, 75–79 (1982)

# A Structural and Magnetic Study of the $CaLa_{1-x}Y_xCrO_4$ System $(0 \leq x \leq 1)$

R. BERJOAN AND J. P. COUTURES

*Laboratoire des Ultra-Réfractaires, Odeillo-Font-Romeu, France*

AND G. LE FLEM AND M. SAUX

*Laboratoire de Chimie du Solide du CNRS, Université de Bordeaux I, 351, cours de la Libération, 33405 Talence Cedex, France*

Received July 21, 1981; in revised form November 17, 1981

Using a solar concentration furnace the $CaLa_{1-x}Y_xCrO_4$ solid solutions were prepared with composition range $0 \leq x \leq 1$. Depending on the yttrium content they belong either to the ideal or to distorted $K_2NiF_4$-type structures. The magnetic properties are characterized mostly by bidimensional antiferromagnetic couplings due to half-filled $t_{2g}$ orbitals of $Cr^{3+}$, but for $x = 1$ the rather covalent Y–O bonds give rise to three-dimensional-type interactions.

The $K_2NiF_4$-type structure may be described as a sequence of layers of tetragonally distorted octahedra, alternating with $K^+$ ions. The separation between the layers is almost twice the intraplanar distance between two $Ni^{2+}$ nearest neighbors (Fig. 1). As a result the interplanar interactions between the magnetic ions are extremely weak, so that magnetic compounds of this type may be generally expected to actually have a two-dimensional behavior (*1*).

Various oxides belonging to the $K_2NiF_4$-type structure have been shown to possess such a 2D-magnetic character (*2, 3*). Were it possible, however, within a solid solution of $K_2NiF_4$ type to reduce gradually the distances between the magnetic layers, this structural evolution would be expected to give rise to progressive appearance of a three-dimensional behavior. In this paper such an approach is illustrated by the structural and magnetic evolution of the $CaLa_{1-x}Y_xCrO_4$ series.

## Preparation

Powders of CaO, $La_2O_3$, $Y_2O_3$, and $Cr_2O_3$ were mixed in stoichiometric proportions. The mixture was melted using a vertical-axis solar furnace described elsewhere (*4*). The samples were placed on a water-cooled aluminum hearth surrounded by a 5-liter pyrex globe which was vacuum-tight sealed. Many preliminary attempts were carried out by varying the atmosphere (argon or argon–hydrogen mixtures) and the melting time to obtain pure phases according to the reaction

$$2\,CaO + (1 - x)La_2O_3 + x\,Y_2O_3 + Cr_2O_3 \rightarrow 2\,CaLa_{(1-x)}Y_xCrO_4.$$

The proportion of hydrogen present in the melting atmosphere was increased with

0022-4596/82/040075-05$02.00/0

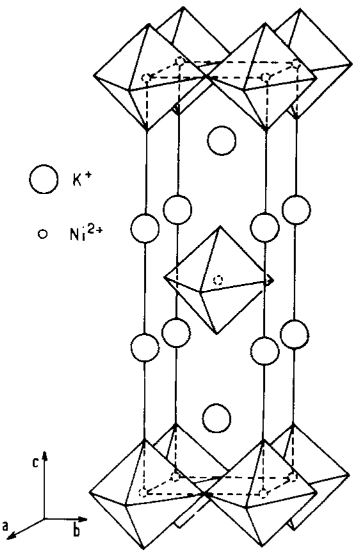

FIG. 1. The $K_2NiF_4$-type structure.

the La content: 0.5% for $x = 1$, but 3% for $x = 0$.

The reaction was carried out twice for 12 sec at about 1900°C. The obtained products were cooled down by pushing the hearth out from the focus of the mirror. The cooling rate was about 250°C/sec in the liquid state and 100°C/sec in the solid state. The melting point measured by infrared pyrometry was about 1800 ± 30°C. After cooling, the materials appeared as green hemispheric globules.

## Structural Study

The $CaLa_{(1-x)}Y_xCrO_4$ solid solution has a composition range of $0 \leq x \leq 1$. Traces of CaO and $La_2O_3$ were detected in the powder diffraction spectra only near $x = 0$. The variation of the lattice parameters with composition is given in Fig. 2, the values being collected in Table I. Their order of magnitude indicates that all solid solutions belong to an ideal or distorted $K_2NiF_4$-type structure. At room temperature three different structures were observed:

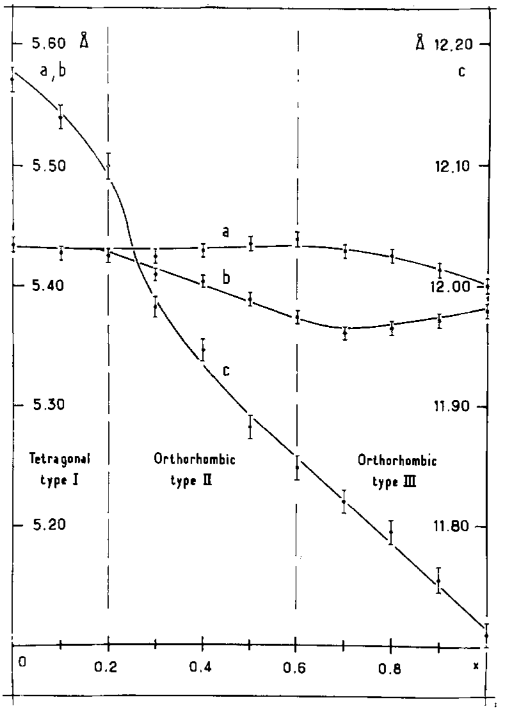

FIG. 2. Variation of the unit cell parameters of $CaLa_{1-x}Y_xCrO_4$.

— for $0 \leq x \leq 0.2$ the unit cell is tetragonal and the condition for possible reflections $h + k + l = 2n$ involves a body-centered lattice (type I);

TABLE I

CRYSTALLOGRAPHIC DATA OF $CaLa_{1-x}Y_xCrO_4$ ($0 \leq x \leq 1$)

| $x$ | $a \pm 0.005$ (Å) | $b \pm 0.005$ (Å) | $c \pm 0.01$ (Å) |
|---|---|---|---|
| 0 | 3.843 ($a(2)^{1/2} = 5.434$) | | 12.17 |
| 0.1 | 3.838 ($a(2)^{1/2} = 5.427$) | | 12.14 |
| 0.2 | 3.837 ($a(2)^{1/2} = 5.426$) | | 12.10 |
| 0.3 | 5.426 | 5.410 | $11.98_5$ |
| 0.4 | 5.430 | 5.405 | 11.95 |
| 0.5 | 5.436 | 5.390 | 11.88 |
| 0.6 | 5.440 | 5.376 | 11.85 |
| 0.7 | 5.430 | 5.362 | 11.82 |
| 0.8 | 5.426 | 5.366 | 11.79 |
| 0.9 | 5.424 | 5.372 | $11.75_5$ |
| 1 | 5.400 | 5.380 | 11.71 |

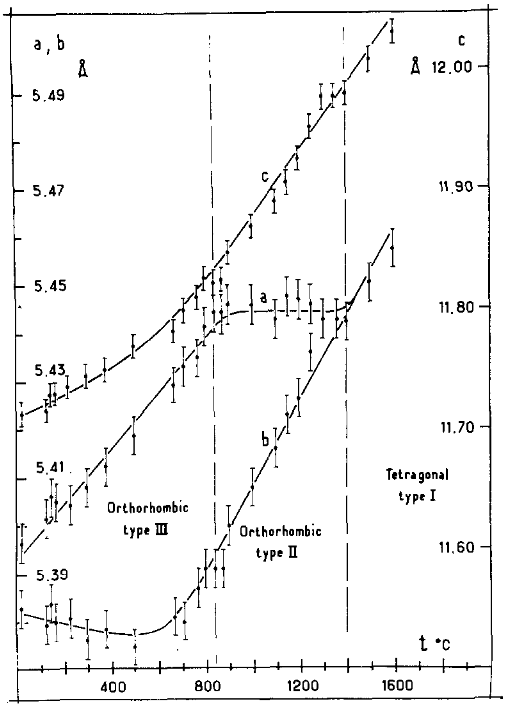

FIG. 3. Thermal variation of the parameters of $CaYCrO_4$.

— for $0.2 \leq x \leq 0.6$ the unit cell becomes orthorhombic and the lattice is face centered. The reflections may exist for $h + k = 2n$, $k + l = 2n$, and $l + h = 2n$ (type II);

— type III appears for $0.6 < x \leq 1$. The unit cell is again orthorhombic, but the condition for reflections becomes $h + k = 2n$.

The $Cr^{3+}$ ions are located in the octahedra and the $Ca^{2+}$, $La^{3+}$, and $Y^{3+}$ ions are randomly distributed between the layers in C.N. 9 sites as it is usually observed for isostructural compounds (*5*, *6*, *11*). In the composition range of type II, the structural evolution is similar to that previously observed for the isostructural $CaLnCrO_4$ and $CaLnFeO_4$ oxides (*5*, *6*): the orthorhombic distortion increases with decreasing average size of the rare earth.

An opposite structural behavior is observed for type III. As $x$ increases the distortion seems to disappear, and the symmetry of the lattice tends progressively to a tetragonal one. In order to explain this new distortion type the thermal variation of the cell parameters of $CaYCrO_4$ ($x = 1$) were examined in a high-temperature X-ray diffractometer. The finely ground samples were deposited on a rhenium ribbon acting as a heating element. The atmosphere in the camera was a mixture of helium with 2% hydrogen. The temperature of the sample

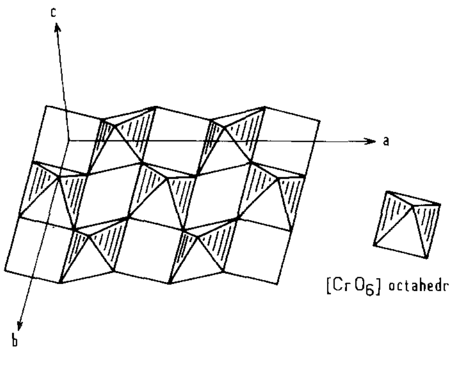

FIG. 4. Tilting of $CrO_6$ octahedra in type III $CaYCrO_4$.

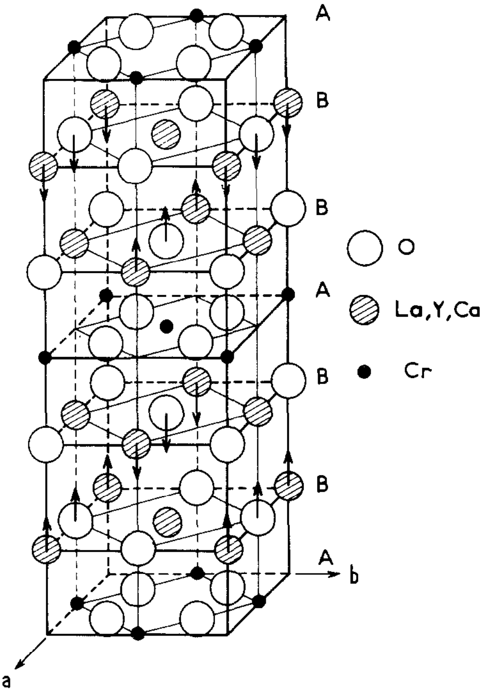

FIG. 5. The structure of $CaYCrO_4$ (type II).

was measured by a fine Pt–PtRh 10% thermocouple welded on the ribbon for temperatures up to 900°C and by an optical micropyrometer working at 0.64 μm between 900 and 1600°C. The results are plotted in Fig. 3. The *a* parameter increases regularly up to about 840°C, remains constant between 840 and 1400°C, and then increases linearly with temperature. The *b* parameter, which is smaller than *a* at room temperature, is roughly constant up to about 700°C and then increases up to 1400°C, where it merges in *a*. The *c* parameter rises in the whole temperature range.

The indexing of the X-ray diffractograms shows two reversible allotropic transformations: around 840°C a type III $\rightleftarrows$ type II transition followed by a type II $\rightleftarrows$ type I transition at 1400°C. The parallel evolution of the structures with decreasing $x$ and rising temperature allows us to formulate the following hypothesis.

At room temperature, as $x$ exceeds 0.6, the observed decrease of the *a* parameter could be due to an antiparallel tilting of two near-neighbor octahedra around a direction parallel to the *b* axis, as shown in Fig. 4. It is a consequence of the small size of the $Y^{3+}$ ions between the layers. At rising temperature, the tilted octahedra again take progressively their normal symmetrical positions. Around 840°C this canceling distortion gives rise to a type III → type II transition.

The type II → type I transition is similar to that previously described for the analogous $Ca_{1+x}Y_{1-x}CrO_4$ series (*7*). The replacement of $La^{3+}$ by $Y^{3+}$ increases the covalency of the rare earth–oxygen bonds. The concerned atoms become closer with rising $x$. As shown by the arrows in Fig. 5, the rare earth cations and the oxygen anions between the octahedra layers move along the *c* axis, leading to an orthorhombic distortion. When the temperature is raised, this attraction is weakened and the structure goes over to the tetragonal type I symmetry due to an increase of the *b* parameter, *a* remaining constant.

## Magnetic Properties

The magnetic properties were studied for samples corresponding to $x$ = 0.4, 0.5, 0.7, and 1. The magnetic susceptibility measurements were performed using a Foner magnetometer and a Faraday balance between 4 and 800 K. The experimental data were corrected from the diamagnetic contributions.

The thermal variation of the reciprocal susceptibility is reported in Fig. 6. For the first three compositions, the curves seem to be characterized by a two-dimensional magnetic behavior: they show a broad minimum and become progressively linear at high temperature. Conversely, the curve obtained for $CaYCrO_4$ ($x$ = 1) is similar to that previously reported for $Ca_2MnO_4$ (*8*). The rather sharp minimum which appears around 120 K implies significant superexchange interplanar interactions. The magnetic data are given in Table II.

The observed Curie constants are higher than the value calculated from the spin-only contribution with $S = \frac{3}{2}$ ($C$ = 1.875). Nevertheless, they become closer as $x$ increases. The exchange integrals were calculated using the Rushbrooke and Wood equations (*9*) adapted by Lines (*10*) and corresponding to two-dimensional interactions of the

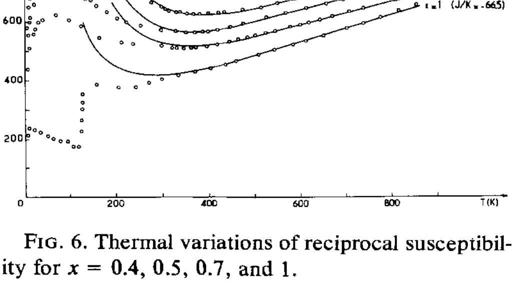

FIG. 6. Thermal variations of reciprocal susceptibility for $x$ = 0.4, 0.5, 0.7, and 1.

TABLE II

MAGNETIC DATA RELATIVE TO $CaLa_{1-x}Y_xCrO_4$ SOLID SOLUTIONS

| $x$ | $\theta_p$ (K) | $C_{exp.}$ | $J/k_B$ (K) |
|---|---|---|---|
| 0.4 | −1020 | 2.44 | −99 |
| 0.5 | −855 | 2.33 | −91 |
| 0.7 | −780 | 2.29 | −85 |
| 1 | −490 | 2.02 | −66.5 |

Heisenberg type with a square planar geometry. This model can describe the magnetic behavior only at high temperature (*12*). The calculated susceptibilities were in good agreement with the experimental data over a large temperature range. $|J/k_B|$ decreases with rising $x$.

## Discussion of the Magnetic Properties

In the $CaLa_{1-x}Y_xCrO_4$ phases, the strongest magnetic couplings occur obviously inside the layers containing the $Cr^{3+}$ ions. They are antiferromagnetic due to the half-filled $t_{2g}$ orbital.

$|J/k_B|$, which characterizes the strength of the couplings, drops with increasing $x$: as the Y–O bonds are more covalent than the La–O bonds, the competing Cr–O bonds weaken. Therefore, the magnetic interactions between nearest-neighboring $Cr^{3+}$ ions must decrease.

For $CaYCrO_4$, by analogy with $Ca_2MnO_4$, the minimum observed around 120 K can be considered as being approximately a Néel temperature (*8*). The Stanley Kaplan temperature calculated from (*10*) ($T_{SK}$ = 130 K) is only slightly higher than the ordering temperature. As we have recently shown, such a behavior is due to the appearance of three-dimensional interactions (*1*). $CaYCrO_4$ has the maximum yttrium content ($x$ = 1) and as a result, the minimum interplanar distance (Fig. 2). The three-dimensional coupling likely occurs due to relatively more covalent Y–O bonds along the $c$ axis.

## References

1. G. LE FLEM, P. COURBIN, C. DELMAS, AND J. L. SOUBEYROUX, *Z. Anorg. Allg. Chem.* **476**, 69 (1981).
2. MM. NGUYEN-TRUT-DINH, M. VLASSE, M. PERRIN, AND G. LE FLEM, *J. Solid State Chem.* **32**, 1 (1980).
3. J. L. SOUBEYROUX, P. COURBIN, L. FOURNES, D. FRUCHART, AND G. LE FLEM, *J. Solid State Chem.* **31**, 313 (1980).
4. J. P. COUTURES, R. BERJOAN, G. BENEZECH, P. GRANIER, R. RENARD, AND M. FOEX, *Rev. Int. Hautes Temp. et Refract.* **15**, 103 (1978).
5. A. DAOUDI AND G. LE FLEM, *Mater. Res. Bull.* **8**, 1103 (1973).
6. A. DAOUDI, Thèse de Doctorat ès-Sciences, Université de Bordeaux I (1974).
7. C. CHAUMONT, G. LE FLEM, AND P. HAGENMULLER, *Z. Anorg. Allg. Chem.* **470**, 18 (1980).
8. G. OLLIVIER, Thèse de Doctorat ès-Sciences, Université Scientifique et Médicale, Grenoble (1973).
9. G. S. RUSHBROOKE AND P. J. WOOD, *Mol. Phys.* **1**, 257 (1958).
10. M. E. LINES, *J. Phys. Chem. Solids* **31**, 101 (1970).
11. K. SANDER, U. LEHMANN, AND H. MULLER-BUSCHBAUM, *Z. Anorg. Allg. Chem.* **480**, 103 (1981).
12. D. H. MARTIN, *In* "Magnetism in Solids," Iliffe, London (1967).